Interaction of Organic Molecules with the TiO_2 (110) Surface: Ab Inito Calculations and Classical Force Fields

Maria L. Sushko,* Andrey Yu. Gal, and Alexander L. Shluger

Department of Physics and Astronomy, University College London, Gower Street, London WC1E 6BT, United Kingdom

Received: September 27, 2005; In Final Form: January 9, 2006

We have studied the adsorption of a number of organic molecules consisting of methyl, benzyl, and carboxylic groups on the rutile TiO_2 (110) surface using both ab initio and atomistic simulation techniques. We have tested the applicability of a simple embedded cluster model to studying the adsorption of small organic molecules on the perfect rutile TiO_2 (110) surface, and used this model to develop a classical force field for the interactions of a wide class of organic molecules consisting of these groups with the rutile TiO_2 (110) surface. The force field accounts for physisorption and ionic bonding of organic molecules at the surface. It allows the reproduction of adsorption energies and of geometries of organic molecules on the rutile surface. It should be useful for studying diffusion of these molecules and their manipulation with use of AFM and STM tips.

1. Introduction

Understanding the mechanisms of adsorption and diffusion of organic molecules at insulating surfaces is important fundamentally and for many potential applications in chemistry and nanotechnology (see for example refs 1−4). This understanding can be greatly enhanced by imaging molecules at surfaces with use of scanning probe methods. Our long-term goal is to establish the interactions governing adsorption, imaging, and manipulation of organic molecules at oxide surfaces, combining theoretical modeling with experimental studies with Atomic Force Microscopy (AFM). The TiO_2 (110) surface is among the most widely used substrates due to both well-established procedures for obtaining high quality surfaces and a wide range of applications. The narrow band gap of reduced TiO_2 samples allows one to employ both Scanning Tunneling Microscopy (STM) and AFM techniques to study the same system. These and other surface techniques provide ample information about the structure and properties of surfaces and adsorbed systems (see, for example, a recent review by Diebold[5]) but often require theoretical modeling to reach a detailed understanding.

Atomistic theory of adsorption and AFM imaging of organic molecules both face the generic problem of describing the interaction between inorganic materials, comprising substrates and AFM tips, with organic molecules. Recently, some of the related issues have been discussed in conjunction with ab initio modeling of AFM imaging of monolayers of formate, acetate, and trifluoroacetate on the rutile surface.[6] The adsorption of several organic molecules at TiO_2 surfaces has been studied in a series of works[7−9] with various quantum-chemical methods. However, due to the large dimensions of molecule/surface/tip systems, fully ab initio and even semiempirical quantum mechanical modeling of such systems is often very challenging and time consuming. Therefore other theoretical methods, such as atomistic simulations with classical interatomic potentials, have to be used. Here, reliable force fields describing the interactions of organic molecules with the inorganic polar materials of the tip and the substrate are crucial. Such force fields are currently unavailable for most molecule/surface/tip combinations. One of the reasons for this is that constructing a simple and universal force field is extremely challenging due to the varying character of carbon hybridization in different types of molecules and their diverse electronic structures. In this paper we consider the interaction of molecules belonging to the group of aliphatic and monocyclic aromatic hydrocarbons, ethers, and carboxylic acids with perfect rutile (110) surface. These include methane, formic acid, benzene, *m*-xylene, dimethyl ether, benzoic acid, and bibenzoic acid. As a prototype large system we consider the $C_{52}H_{72}O_3$ molecule shown in Figure 1. This molecule has been synthesized at CEMES CNRS and is currently being used as a test system for AFM manipulation on the TiO_2 surface.[10] We are aiming at exploring the mechanisms of adsorption of these molecules and the ways of deriving classical force fields for describing adsorption of this and similar systems on oxide surfaces. We note that the strength and even the mechanism of adsorption on reduced surfaces can differ from that on a perfect substrate. However, the method for the force-field construction proposed in the present paper can also be applied to reduced surfaces with established composition and structure.

Force-field parameters for the interaction of H_2O and pyridine and its derivatives with the TiO_2 (110) surface have been obtained in refs 11 and 12, respectively. These studies employed ab initio calculations of the interaction of molecules with small clusters modeling the TiO_2 surface. More generally, force fields for modeling the interactions between some organic and inorganic systems are available in the commercial COMPASS software.[13−15] Similar problems have recently been considered in the context of modeling inhibiting effects of organic adsorbates on calcite crystal growth.[16,17] We are aiming at considering much bigger organic molecules at the TiO_2 (110) surface and other oxide surfaces. We demonstrate that some such molecules can be divided into smaller molecular fragments for force-field derivation. The parameters of the force field describing the interaction of these fragments with the surface

* Address correspondence to this author. E-mail: m.sushko@ucl.ac.uk.

10.1021/jp055486q CCC: $33.50
Published on Web 02/15/2006

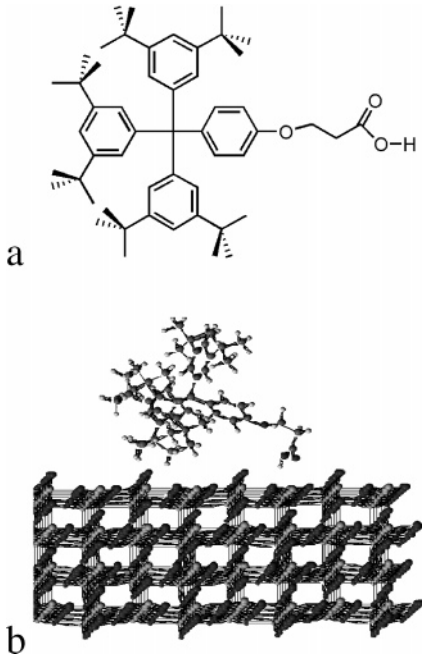

Figure 1. The chemical structure (a) and one of the stable configurations of the $C_{52}H_{72}O_3$ molecule on TiO_2 surface (b).

can be obtained by using ab initio calculations and pairwise potential approximation, and then the force field for the big molecule/surface system can be obtained by summing up the pair potentials for individual constituent atoms. This approach predicts the adsorption energies and geometries for an array of test hydrocarbon molecules in good agreement with the experimental data and the results of ab initio calculations.

The paper is organized as follows. In the next section we describe our approach to deriving the parameters of the classical force field. In section 3 we present the quantum mechanical methods used for calculating the interaction of molecules with the rutile surface. In section 4 we discuss the mechanism of adsorption of small organic molecules on TiO_2 surface, and in section 5 we discuss the derivation and the testing of the force field. The discussion and conclusions are presented in section 6.

2. Method of Force-Field Construction

In this paper we carry out ab initio calculations for the adsorption of an array of organic molecules on the rutile surface and explore whether it is possible to construct a reliable full molecule + surface force field by breaking a big molecule into simpler molecules, fitting a force field for the interaction of each of these smaller molecules with the surface using pairwise interactions, and then calculating the interaction of the big molecule with the surface as a sum of pairwise potentials derived for small molecules. The potential advantage of this approach is that the interaction of small molecules with the surface can be treated with ab initio methods. The quantum mechanical force field obtained then can be approximated by a sum of pairwise interatomic potentials between the molecule and surface atoms. The interactions between atoms inside the big molecule and within the surface, in their turn, can be treated by using standard force fields.[11,18]

In particular, the $C_{52}H_{72}O_3$ molecule shown in Figure 1 consists of 3,5 isobutyl phenyl headgroups (derivatives of *m*-xylene) and an ethyl formate tail group. The location of these groups with respect to the surface depends on the orientation of the big molecule and can be very far from the equilibrium adsorption site for each particular group. Therefore, for modeling adsorption, AFM imaging, and probing different manipulation mechanisms, the force field should reproduce the energies and geometries of adsorbed molecules not only at the most stable but also at various other positions at the surface. These are our main criteria for the quality of the derived force field.

Since we consider the small molecules as building blocks of a more complex molecule, one or more hydrogens in the CH_4, C_6H_6, or HCOOH molecules effectively simulate the presence of the rest of the big molecule. On re-assembling a big molecule, these hydrogens are removed and substituted by the relevant groups of larger molecules. For example, an H atom of a CH_4 molecule and an H atom of a C_6H_6 molecule might be removed and the resulting CH_3 group attached to C_6H_5. We also have to take into account the change of the charging states of the carbons forming the C−C bond, which ensures the overall neutrality of the formed molecule. The above procedure is only valid if this reassembly does not significantly affect the interactions of the constituent atoms with the surface. For this approach to be feasible, it is also important that the interactions of the functional groups with the surface are not coupled to each other and, therefore, could be considered independently. This may be valid when there is no significant electron transfer between the organic molecule and the surface.

3. Methods of Calculations

To calculate the geometric and electronic structures of the rutile (110) surface and to examine the interaction of molecules with this surface we used two models and computational techniques. Fitting a versatile force field requires consideration of the interaction of molecules with the surface for a wide range of distances and configurations. Using a cluster model allows us to calculate these interactions efficiently. To test the applicability of the cluster model and the derived force field we used periodic calculations.

3.1. Cluster Model. The surface and bulk rutile TiO_2 were modeled with Ti_nO_m clusters saturated by pseudohydrogens. The charges on pseudohydrogens were calculated according to the formal charges of Ti and O and their coordination number in the bulk, as proposed by Casarin et al.[19] Since in the rutile structure Ti is 6-fold coordinated and O is 3-fold coordinated, meaning each Ti shares its four valence electrons with 6 oxygen atoms, the pseudohydrogen saturating the dangling bond of oxygen (H′) has a charge of $^1/_6q(\mathrm{Ti}) = {}^2/_3\ |e|$, where q(Ti) is the formal charge of the Ti ion. Similarly, the charge of the pseudohydrogen saturating Ti (H″) is $^1/_3q(\mathrm{O}) = -{}^2/_3\ |e|$. The formal Ti and O charges are $+4\ |e|$ and $-2\ |e|$, respectively, and $|e|$ is the electron charge. Pseudohydrogens were positioned along the bond directions of the extended lattice. The distances of pseudohydrogens from O and Ti ions were determined via optimization of the OH'_3 and TiH''_6 pseudomolecules, respectively (Figure 2). This model has been shown to be accurate enough for modeling the adsorption of small molecules at the center of the cluster.[19]

Cluster calculations were performed with both the Hartree−Fock (HF) method and the Density Functional approach (DFT) with a hybrid density functional B3LYP[20,21] implemented in the Gaussian98 code.[22] To allow for the noninteger charges of pseudohydrogens we used the following embedding procedure: the quantum cluster terminated by quantum hydrogens with formal charges equal to $+1\ |e|$ for H′ and $-1\ |e|$ for H″, respectively, was embedded into an array of classical charges positioned on hydrogens to achieve the desired total charge of pseudoatoms as described above. This embedding procedure can

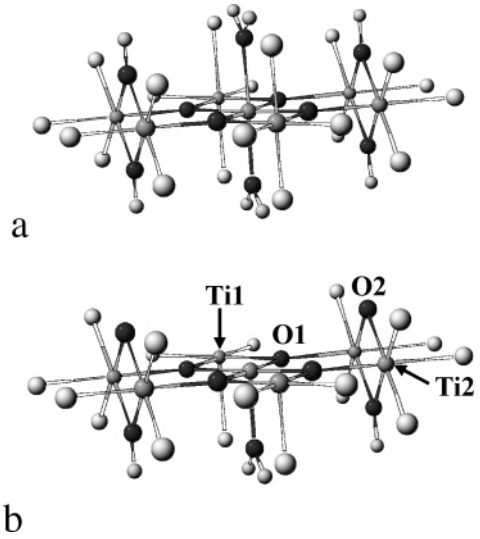

Figure 2. Clusters representing (a) "bulk" rutile, Ti_7O_{10}, and (b) the rutile (110) surface, Ti_7O_9, used in most calculations. The following notations are used: black spheres, O; small light gray spheres, Ti; large white spheres, H′; and small white spheres, H″. The larger Ti_7O_{18} and Ti_7O_{30} clusters were constructed by using the same principle via substitution of part or all of the H″ by oxygens and saturation of oxygens dangling bonds with H′.

be realized within the GUESS (Gaussians Used for Embedded System Studies) code,[23,24] which interfaces the Gaussian98 package[22] for quantum mechanical calculations with a program for classical calculations.

To choose the basis set, we studied the basis set dependence of the electronic properties of stoichiometric clusters Ti_7O_{10}, Ti_7O_{18}, and Ti_7O_{30} representing the bulk TiO_2 (see Figure 2). Note that for simplicity of notation we omit the interfacial atoms in the names of the clusters. Three basis sets were considered: 3-21G(d) for all atoms, 6-31G(d) for all atoms, and 86−411-(d31)G for Ti with 6-31G(d) for O atoms. We found that HF calculations with all three basis sets give similar band gap widths as well as similar effective charges on the corresponding ions of the cluster calculated by using Natural Population Analysis (NPA). We used the 6-31G(d) basis set in all further calculations.

3.2. Periodic DFT Calculations. Periodic calculations were performed with the SIESTA package.[25,26] It employs the density functional theory within the Generalised Gradient Approximation (GGA) and the Perdew, Burke, and Ernzerhof (PBE) exchange-correlation functional. The Troullier−Martins pseudopotentials were generated in the electronic configurations $[1s^2]$ $2s^2$ $2p^4$, $[1s^2]$ $2s^2$ $2p^2$, [Ne] $3s^23p^63d^2$ for O, C, and Ti atoms, respectively. Square brackets denote the core electron configurations. The pseudopotentials were constructed on the basis of the solution for free atoms, using the PBE functional.

We used the Numerical Atomic Orbitals (NAO) basis sets in all calculations. The details of NAO generation are extensively described elsewhere.[25,27] To reduce the computational effort, the atoms representing the deepest TiO_2 layer in the slab are described with a "single-ξ" basis set following previous studies of the TiO_2 (110) surface.[6] The basis set includes s- and p-orbitals or s- and d-orbitals for both ions obtained from the solution of the atomic problem. The accuracy of the real-space mesh is characterized by the energy cutoff of 150 Ry, which corresponds to a real-space mesh step of 0.16 Å. The basis set was gradually increased until the band gap reached 0.8 eV and the addition of an extra basis function resulted in less than 0.1 eV increase in the band gap.

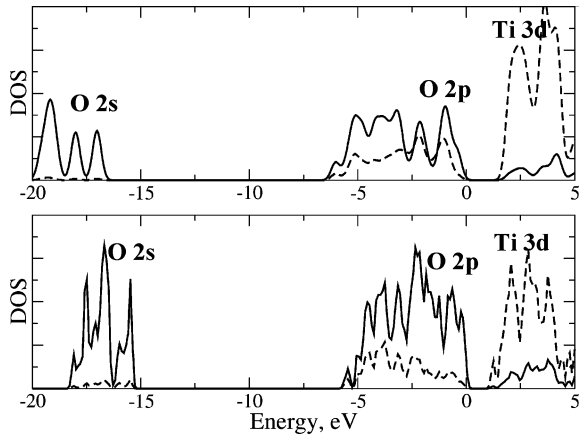

Figure 3. Projected density of states of the TiO_2 (110) surface. For comparison PDOS's obtained in a cluster (Ti_7O_{10} cluster, B3LYP method) (upper graph) and periodic (their layer slab, DFT-GGA method) (lower graph) models are shown. The solid line corresponds to the PDOS of oxygen and the dashed line to the PDOS of titanium.

The surface calculations are carried out in a 3-dimensional periodic slab model. The lateral size of the unit cell was fixed according to the optimized bulk geometry. In particular, the (2 × 2)-expanded surface unit cell has lateral dimensions of 6.03 × 6.72 Å, which are slightly bigger than the values of 6.0 × 6.5 Å experimentally defined in AFM measurement.[28] The 3-layer slab was used as the primary model in further TiO_2 (110) surface calculations. The interslab interaction, which may affect the results of adsorption calculations, was reduced by increasing the gap between the slabs up to 20 Å. The interaction between the slabs with adsorbed formic acid molecules was estimated to be less than 0.02 eV.

3.3. Tests of the Cluster Model. To compare the electronic properties of the clusters with the available experimental and theoretical data for bulk TiO_2 and the (110) surface and to test their dependence on the cluster size and saturation we used DFT calculations with the B3LYP functional.[20,21] The latter is known to give accurate band gaps for a wide number of solids and surfaces[29] and thus allows direct comparison with experiment. In the clusters representing the rutile TiO_2 bulk and surface (Figure 2), the saturation of the border Ti ions is different. In the bulk Ti_7O_{10} and Ti_7O_{18} clusters as well as in the surface Ti_7O_9 and $Ti_{10}O_{16}$ clusters, the Ti ions are partially surrounded by quantum oxygens and partially by pseudohydrogens, while in the bulk Ti_7O_{30} cluster all Ti ions are surrounded by quantum oxygens. Therefore we are probing the convergence of the electronic properties not only with the size of the cluster but also with the method of saturation. The band gap obtained in these cluster calculations is about 3.0 eV for the bulk and 2.4 eV for the surface. The band gap for the bulk rutile agrees well with the experimental value[30] of 3.05 eV. Almost no dependence of the band gap on the cluster size was observed.

Comparison of the projected densities of states (DOS) for the cluster and periodic DFT calculations provides an additional test of the cluster model. The width of the upper valence band as well as the gap between the upper and lower valence bands for the clusters representing the surface (Figure 3) agree fairly well with the experimental data.[31,32] The main contribution to the lower valence band is given by the O 2s orbitals, the upper valence band is mostly associated with O 2p orbitals, while the bottom of the conduction band is largely composed of the Ti 3d orbitals (Figure 3). However, in the cluster calculations, the Ti states contribute more strongly to the top of the valence band than in periodic calculations. The oxygen 2p orbitals still provide

TABLE 1: Relaxation of the Rutile (110) Surface[a]

	cluster, HF		periodic, DFT		experiment[33]	
atom	*x*, Å	*z*, Å	*x*, Å	*z*, Å	*x*, Å	*z*, Å
Ti1	0.00	−0.23	0.01	−0.14	0.00	−0.16 ± 0.05
Ti2	0.00	0.07	0.01	0.19	0.00	0.12 ± 0.05
O1	−0.15	0.03	−0.05	0.15	−0.16 ± 0.08	0.05 ± 0.05
O2	0.01	−0.06	0.02	−0.04	0.00	−0.27 ± 0.08

[a] The following notations are used: Ti1 is in-plane Ti; Ti2 is Ti bound to the bridging oxygen; O1 is in-plane O; and O2 is the bridging O (see Figure 2b).

the main contribution to the upper valence band. Therefore, the cluster model gives a reasonably good representation of the electronic structure of the rutile TiO_2 surface.

Numerous experimental and theoretical studies have shown that the rutile TiO_2 (110) surface undergoes substantial relaxation.[33−36] The ability to reproduce this relaxation is vital for studying the adsorption of various molecules at the surface. To study the surface relaxation we used the $Ti_{10}O_{16}$ cluster and the HF method. All ions not directly bonded to the pseudohydrogens were allowed to relax while the rest of the cluster remained fixed in the configuration corresponding to the bulk geometry. The parameters of the calculated surface structure are presented in Table 1 along with the data from our periodic DFT calculations (NAO-PBE) as well as the experimental X-ray diffraction data. The relaxation of Ti and in-plane oxygen atoms is reproduced reasonably well in both cluster and periodic NAO-PBE calculations, while the relaxation of the bridging oxygen is substantially lower than that suggested on the basis of the X-ray data.[33] This effect is characteristic to most available first principle calculations of the rutile (110) surface. A wide variety of density functional methods using localized basis sets (LACO-PBE, PW-LDA, and PW-GGA) (ref 34 and references therein) as well as the HF method give a value for the downward bridging oxygen relaxation of −0.02 to −0.06 Å, while calculations with the full-potential linearized augmented plane wave (FP-LAPW) formalism give a value of oxygen relaxation closer to the experimental one (−0.16 Å) (ref 34). It has been suggested that this discrepancy between theory and experiment is due to the presence of soft anharmonic surface vibrational modes, which are not taken into account in first principle calculations. It has been shown that these vibrations involve the displacement of surface ions by as much as 0.15 Å at room temperature.[34]

To test the effect of the method on the adsorption properties of organic molecules, we have compared the adsorption curves for methane on the TiO_2 surface obtained using HF and B3LYP methods. The band gap of the TiO_2 surface is three times higher in HF calculations than it is in B3LYP. This can affect the chemical bond formation due to electron transfer between the molecule and the surface. However, as one can see in Figure 4, the adsorption curves obtained by using the two methods almost coincide with each other. The deviation in the adsorption energies is less than 0.02 eV. Therefore, to increase the speed of calculations, the HF method was used to model the adsorption of molecules, which do not form covalent bonds with the surface.

Since the electrostatic forces strongly contribute to the interaction of organic molecules with the rutile surface, it is crucial that the surface model describes correctly the behavior of the rutile electrostatic potential. The cluster boundaries may significantly affect the potential above the surface, especially at large distances. To test this point we compared the electrostatic potential above the Ti_7O_9 cluster representing the surface

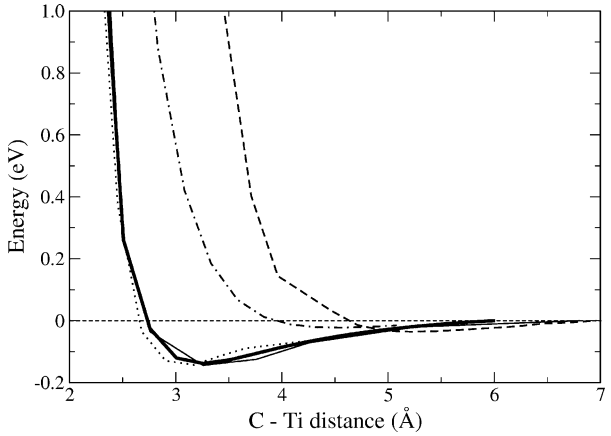

Figure 4. Adsorption of methane on the TiO_2 surface. Adsorption curves of methane with two CH bonds facing the surface over the in-plane Ti (thick and thin solid lines, cluster HF and B3LYP calculations, respectively; dotted line, periodic DFT calculations), over the in-plane O (dot−dashed line, cluster HF calculations), and over bridging O (dashed line, cluster HF calculations).

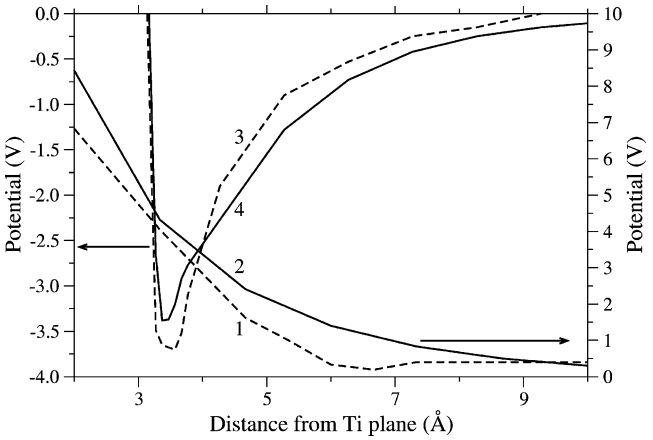

Figure 5. Electrostatic potential above the rutile (110) surface. Curves 1 and 2 correspond to the potential above in-plane Ti and curves 3 and 4 correspond to the potential above the bridging O of the surface. The solid lines correspond to the results of periodic HF calculations and the dashed lines to the results of cluster HF calculations in the Ti_7O_9 cluster. The distances are measured from the Ti plane.

with the potential calculated in the periodic model and the CRYSTAL code.[37] In this model the surface was represented by a three-layer slab periodically translated in two dimensions. Both cluster and periodic calculations of the electrostatic potential were performed with the HF method and the 86-411-(d31)G basis set for Ti and the 6-31G(d) basis set for O ions. As one can see in Figure 5, the deviation of the potential, above the main sites of the surface (bridging O and in-plane Ti and O), obtained in the cluster model from the results of periodic calculations is of the order of 0.3 V in the distances of range 2.0−7.0 Å above surface sites relevant to the study of adsorption. More significant deviations (approximately 0.8 V) are observed for the potential above the bridging oxygen just before the point where the potential changes sign (3.0−3.35 Å above the Ti plane or 1.65−2.0 Å above the bridging oxygen), and in the region of 6.0−7.0 Å above in-plane Ti ions. Again, this is the region where the curvature of the cluster potential curves changes and the potential becomes constant and equal to 0.4 V, while in the periodic model the potential decays to zero. This result indicates that the cluster boundaries can affect the potential of the cluster at distances exceeding 7 Å above the surface. However, as will be shown below, the adsorption

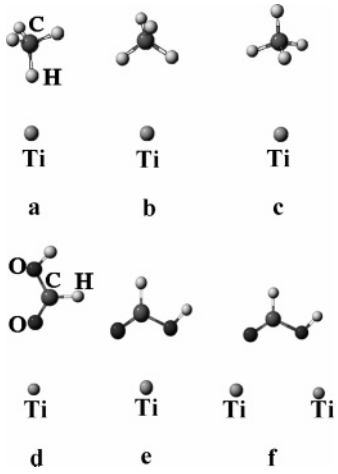

Figure 6. Configurations of methane and formic acid above in-plane Ti sites. The configurations of methane with one (a), two (b), and three (c) CH bonds facing the surface as well as mono- (d) and bidentate 1−2 (e, f) configurations of formic acid are shown.

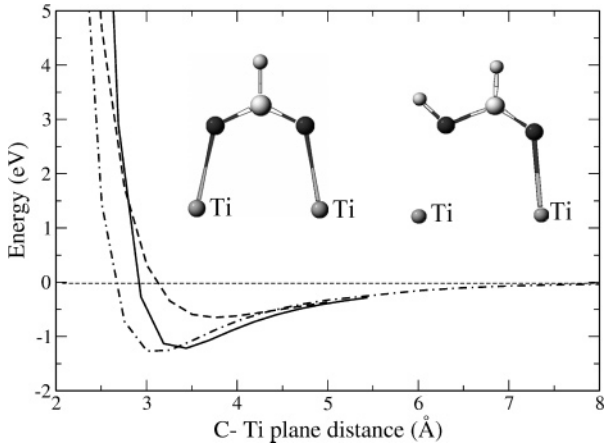

Figure 7. Adsorption curves of the formic acid on the TiO_2 surface. The solid line corresponds to the adsorption in monodentate configuration, while dashed and dot−dashed lines correspond to the adsorption in bidentate 1 and 2 configurations, respectively. The optimized adsorption geometries of formic acid and formate on the TiO_2 surface are shown on the insert.

energies of organic molecules become negligibly small at these distances. Therefore the cluster model can be used for deriving the force field.

The efficiency of the calculations is important for obtaining a sufficient number of energy/distance curves for the interaction of small molecules with the surface for reliable force-field construction. On the basis of the tests described above, to minimize the computational time the calculations of adsorption were carried out with the Ti_7O_9 cluster and the HF method.

4. Adsorption of Small Molecules on the TiO_2 Surface

In this section we consider the interactions of methane, formic acid, and benzene with a perfect rutile (110) surface.

4.1. Adsorption of Methane on the TiO_2 (110) Surface. We have performed HF calculations of the potential energy/distance curves for a methane molecule above the TiO_2 surface. In-plane Ti, in-plane O, and bridge O were considered as the adsorption sites. For all sites, four configurations of the methane molecule with respect to the surface, namely configurations with 1, 2, or 3 CH bonds facing the surface (configurations a, b, and c, respectively), as well as the tilted configuration, were studied (Figure 6). We have found that in all configurations considered the interactions of methane with the surface over the in-plane oxygen site are purely repulsive. The interaction of methane with the surface over bridge oxygen site in configurations a and b is also repulsive. However, a weak attraction was found for CH_4 over the Ti site in all configurations as well as over the bridging oxygen site in the configuration with 2 CH bonds facing the surface. The fully optimized configuration corresponds to the adsorption in configuration b over the Ti ion with the lower CH bonds oriented perpendicular to the Ti row and the upper CH bonds parallel to it.

To test the effect of boundary conditions, the results of the cluster HF calculations were compared with the results of periodic DFT calculations by using the SIESTA code. In periodic calculations the surface was modeled with a (2×1) unit cell 3 layers deep and a spacing between the slabs of at least 2 nm. The methane molecule was oriented with two CH bonds facing the surface (configuration b).

The adsorption energies are almost the same in both calculations and equal to 0.140 and 0.143 eV in the cluster and periodic models, respectively. The shape of the adsorption curves at separations larger than the equilibrium distance is also very similar in both models (Figure 4). The maximum deviation of the adsorption curves obtained by using the cluster and periodic models corresponds to the repulsive part of the curves and is less than 0.12 eV.

Although there is no charge transfer between the methane molecule and the surface, the molecule becomes slightly polarized due to the redistribution of the charge density within the molecule. In particular, in the optimized configuration the Mulliken charges of hydrogens facing away from the surface become 0.21 |e|, compared to 0.16 |e| for a free CH_4 molecule. The negative charge on the carbon ion increases to become −0.71 |e| ($\Delta q = 0.07$ |e| with respect to the free molecule), while the charges on the hydrogens facing the surface remain equal to those in the free molecule. The surface polarization is much smaller. Therefore the molecule polarization is mainly responsible for the attractive force at short molecule/surface separations. However, the interaction is short range with the interaction energy going down to zero at a carbon−in-plane Ti separation of about 4.0 Å (at this distance the corrugation of the surface potential becomes negligibly small). To the best of our knowledge there are no experimental data on the adsorption energy of methane on the rutile surface. The experimental adsorption energy could prove to be higher since our calculations do not fully account for dispersion forces.

4.2. Adsorption of HCOOH on TiO_2 (110). We have considered the adsorption of formic acid in molecular and dissociated (formate) forms. Due to the permanent dipole moment of the molecule, the interactions of the formic acid with the surface are substantially longer range than those for methane (see Figure 7). As in the case of methane adsorption, the surface electrostatic field induces further polarization of the formic acid molecule. However, the net charge redistribution does not exceed 0.2 |e|. Our calculations predict the strongest adsorption in the bidentate 2 configuration with two formic acid oxygens above the surface Ti ions (Figure 6f). The weakest adsorption is in the bidentate 1 configuration, with the adsorption energy in the monodentate configuration between the two (see Figure 6d,e). The obtained adsorption energy of 1.3 eV agrees reasonably well with the results of periodic DFT and HF calculations reported earlier.[38−40] The adsorption mechanism of the formate ion (dissociated formic acid) is similar to that of formic acid. The most favorable configuration is also a bidentate 2 with the dissociated proton forming a covalent bond with a

neighboring bridging oxygen ion in the surface (Figure 7). The adsorption energy is 0.05 eV higher in the dissociated mode and is equal to 1.35 eV.

4.3. Adsorption of Benzene on TiO_2 (110). Different configurations of the benzene molecule, namely parallel and tilted with respect to the surface, situated above different sites at the TiO_2 surface were studied. We note that the Hartree−Fock method used in this study adequately describes the electronic structure of benzene. It has been shown that the HOMO-LUMO gap, the position of the HOMO level, and the nature of the occupied and unoccupied states of benzene obtained in HF calculations are the same as those obtained with use of post-HF methods such as Moller−Plesset perturbation theory, quadratic configuration interaction, and coupled cluster methods.[41] Similarly to the other two molecules, the interaction with the surface induces polarization of benzene. The absolute values of Mulliken charges of the carbon and hydrogen atoms increase by 0.025 |e| to −0.22 |e| for carbon and 0.22 |e| for hydrogen atoms, respectively. However, dipole−dipole and dipole−monopole forces play only a minor role (approximately 20%) in the adsorption of benzene to rutile surface, while the Coulomb interaction between the negative charge distributed on the benzene ring and the positively charged Ti ions of the surface contributes 80% of the interaction energy. Therefore the minimum energy configuration corresponds to the benzene ring parallel to the surface with the center of the ring above the Ti ion. This result agrees well with the previously reported experimental data on the adsorption of benzene on both TiO_2 (110)[12] and (100) surfaces.[42] The polarization of benzene becomes asymmetric in tilted conformations, which leads to an increased role for dipole−monopole forces. However, we find tilted conformations less energetically favorable. The adsorption energy of benzene to TiO_2 surface is substantially lower than that of formic acid and is equal to 0.38 eV, which may also explain the high mobility of benzene along the Ti rows found experimentally.[12]

5. Classical Description of Molecule−Surface Interactions

5.1. Fitting the Parameters. The results of calculations described above demonstrate that there is no charge transfer between the CH_4, C_6H_6, and HCOOH molecules and the TiO_2 surface and the main contribution to the molecule−surface interaction stems from the polarization of molecules in the surface electric field. The formation of derivatives of CH_4, C_6H_6, and HCOOH does not significantly change the electronic structure of the corresponding precursor molecule either. We found that the substitution of two hydrogens of benzene with methyl groups, i.e., the formation of *m*-xylene, lifts the degeneracy of the benzene HOMO level, due to the symmetry reduction, while slightly shifting the HOMO level up. This does not significantly change the effective charges on carbon atoms within *m*-xylene with respect to those in benzene or the character of the molecule−surface interaction. Therefore we believe that it should be possible to describe the interaction between the precursor molecules and the TiO_2 surface with good accuracy using simple pairwise interatomic potentials, and that the parameters of these potentials should be transferable to description of the interaction of more complex derivatives of these molecules and bigger compound molecules with this surface.

Due to these considerations, we impose the following constraint on the short-range part of the C/Ti and C/O_{Ti} (O_{Ti} denotes the oxygen of the surface) pair potentials. The parameters for the pair potentials for carbon should be almost the same for different molecules, i.e., should be independent of the hybridization state of carbon, while the partial charges may vary. This allows accounting for different adsorption mechanisms of methane and benzene molecules. Most importantly the independence of the short-range interactions of carbon with the TiO_2 surface with respect to its hybridization state allows methane or benzene derivatives to be considered in the same way as methane or benzene, respectively. The short-range part of the interactions will stay unchanged while the charges on the carbons covalently bound to some other groups instead of hydrogens will be different. According to ab initio calculations, the variation of charges on these carbon atoms will not be greater than 0.2 |e|. Therefore all the difference in the interaction energy between the surface and the small molecules or their derivatives will be incorporated into the Coulomb part of the interactions. This variation of charges with the hybridization state of carbon is included into the force field used for describing the interactions within the molecule,[18] which makes the whole description consistent. In complex organic molecules the Coulomb part of the interaction with the surface will also become the main part of the interaction for most of the functional groups since the distance of these groups to the surface will be equal or higher than the equilibrium distance for the small molecules representing these groups.

We have constructed a potential energy map for small molecules on the rutile (110) surface over different surface sites for various orientations of the molecules with respect to the surface. The centers of these molecules were positioned above the three main sites on the surface: the in-plane Ti and O ions as well as the bridging oxygen ion. Depending on the symmetry of the molecule, up to 12 orientations with respect to the surface were considered. For each orientation, the energy of the molecule at the TiO_2 surface was calculated for 16 molecule/surface separations. The pair potentials were fitted to reproduce the adsorption curves obtained from quantum mechanical calculations. First, the potentials were fitted to reproduce the adsorption curve corresponding to the most favorable configuration of the molecule on the surface. Then the obtained pair-potential parameters were refined by using the adsorption curves for all other configurations of the molecule. In this second step of the fitting process the maximum weight was assigned to configurations with the lowest energies and the minimum weight to the highest energy configurations. The maximum root-mean-square deviation of the fitted energy−distance curves from the quantum mechanical data was 0.1 eV.

As a first approximation we have used the potentials reported in ref 43 for the interaction of poly(ethylene oxide) with TiO_2 surface, which we refined according to our ab initio results. Both Coulomb and short-range interactions were included in the model. Following the approach used in ref 43 the short-range interactions of Ti and O_{Ti} with organic molecules were described by using 6-12 Lennard-Jones and Buckingham type potentials, respectively. The following forms of potentials have been used:

$$U_{ij}(r_{ij}) = A_{ij}/(r_{ij}^{12}) - B_{ij}/(r_{ij}^{6}) + q_i q_j / r_{ij}$$

for the interactions of the C, H, and O of the organic molecules with the surface Ti ions and

$$U_{ij}(r_{ij}) = A_{ij} \exp(-r_{ij}/\rho_{ij}) - B_{ij}/(r_{ij}^{6}) + q_i q_j / r_{ij}$$

for the interactions of the C, H, and O of the organic molecules with the surface oxygens. The bridge and in-plane oxygens are considered as different species. We would like to note that, since the potentials were fitted to the adsorption curves obtained by

TABLE 2: Pair-Potential Parameters[a] See the Notation for the Ions of the Surface in Figure 2b

molecule	atom types	potential	A, eV or eV·Å^{12}	ρ, Å	B, eV·Å^6	charge
CH_4	C−Ti	Lennard 12−6	5420.40675		27.96900	q(C) = −0.308|e|
	H−Ti	Lennard 12−6	275.84330		1.38760	q(H) = 0.077|e|
	C−O1(2)	Buckingham	1461.44570	0.27956	21.80000	
	H−O1	Buckingham	614.71660	0.27031	4.51000	
	H−O2	Buckingham	614.71660	0.25631	4.51000	
C_6H_6	C−Ti	Lennard 12−6	5420.40675		0.01930	q(C) = −0.195|e|
	H−Ti	Lennard 12−6	275.84330		1.38760	q(H) = 0.195|e|
	C−O1(2)	Buckingham	1461.44570	0.27956	0.01300	
	H−O1	Buckingham	614.71660	0.27031	7.51000	
	H−O2	Buckingham	614.71660	0.24631	7.51000	
HCOOH*	C−Ti	Lennard 12−6	5420.40675		0.01930	q(C) = 0.568|e|
	H3(4)−Ti	Lennard 12−6	275.84330		1.38760	q(O3) = −0.494|e|
	O3(4)−Ti	Lennard 12−6	4233.20750		21.50800	q(O4) = −0.693|e|
O3═C(−H4)−O4−H3	C−O1(2)	Buckingham	2561.44570	0.27956	0.01345	q(H3) = 0.474|e|
	H3(4)−O1	Buckingham	614.71660	0.27031	7.50761	q(H4) = 0.145|e|
	H3(4)−O2	Buckingham	614.71660	0.24631	7.50761	
	O3(4)-−1(2)	Buckingham	3288.87700	0.24612	17.21044	

[a] See the notation for the ions of the surface in Figure 2b. [b] The parameters of the pair potentials for formate are the same as those for the formic acid with the partial charges q(O3) = q(O4) = −0.657 |e| and q(H4) = 0.272 |e|.

the HF method which does not take into account the van der Waals interaction, it is tempting to represent the attraction with a functional form including $B_{ij}/(r_{ij}^4)$ or $B_{ij}/(r_{ij}^2)$ terms to account for the dipole−induced dipole and dipole−monopole interactions, respectively. However, our attempts to fit the adsorption curves by the potential containing these terms gave worse results in the vicinity of the minimum than with the $B_{ij}/(r_{ij}^6)$ term. Therefore we have used the above expressions for the potentials. They are commonly used in atomistic simulations and implemented in most programs for molecular dynamics and molecular mechanics calculations. The interactions inside the organic molecules were described by using the available force field by Cornell et al.[18] while the force field developed by Bandura et al.[11] was used to model the rutile TiO_2 surface.

The classical charges of the surface ions and those inside the molecules were taken to be equal to the slightly scaled Mulliken charges obtained in the HF calculations with the 6-31G(d) basis set. The Mulliken population analysis has been used to retain consistency with the charges used in the force fields for the surface[11] and the organic molecules,[18] respectively. The charges for the surface ions obtained in our calculations agree with those used in the force field for the TiO_2 surface by Bandura et al.[11] within 0.07 |e|. Therefore, to retain the consistency of the atomistic description of the surface, the charges of the original force field have been used. In some cases slight adjustment of the charges (in the range of $q_{\text{Mulliken}} \pm 0.05$ |e|) of organic molecules was performed to fit the long-range part of the molecule/surface interaction. This did not violate the consistency of the force field inside the molecule since the Coulomb interactions are used to describe the intermolecular interactions only.[18]

All atomistic calculations were performed by using the General Utility Lattice Program (GULP).[44] The 3 × 3 and 6 × 6 periodic cells four layers deep were used to model the adsorption of small and large organic molecules, respectively. The conjugate gradient algorithm[45] was used to perform geometry optimization.

The optimized parameters of pair potentials for the interaction of small molecules with the TiO_2 (110) surface are presented in Table 2. For all organic molecules/TiO_2 interactions potentials a 10 Å cutoff was used. The optimized geometries of small molecules on the TiO_2 surface obtained with the derived pair potentials are in good agreement with those from the ab initio calculations (Table 3). The adsorption energies are also well reproduced in atomistic calculations.

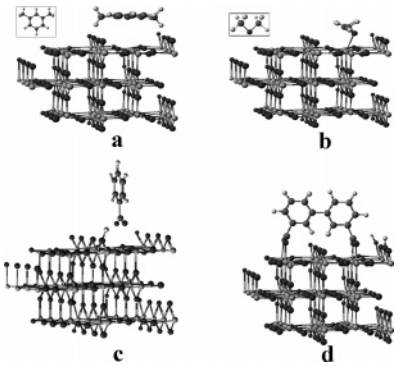

Figure 8. Structure and adsorption geometry of *m*-xylene (a), dimethyl ether (b), benzoic acid (c), and bibenzoic acid (d).

TABLE 3: Comparison of Cluster HF Data on the Adsorption Energy and Adsorption Geometry with the Results of Atomistic Calculations, Using the Derived Force Field

		distance, Å		adsorption energy, eV	
molecule		HF	atomistic	HF	atomistic
CH_4	C−Ti	3.258	3.000	0.138	0.135
C_6H_6	benzene ring−Ti plane	3.931	3.820	0.408	0.4
HCOOH	C−Ti plane	3.005	3.004	1.268	1.269
	O−Ti	2.172	2.170		

5.2. Testing the Potentials. To test the interatomic potentials described above we have compared the results of ab initio and atomistic calculations for adsorption of four larger molecules consisting of methyl, benzyl, and carboxylic groups at the rutile surface. The molecules studied were *m*-xylene, dimethyl ether, benzoic acid, and bibenzoic acid (Figure 8). The ab initio calculations for the first three molecules were performed in a cluster model with the HF method. In these calculations the surface was represented by an extended $Ti_{10}O_{16}$ cluster to minimize the interference of the cluster boundaries. Bibenzoic acid is too large to be studied in a cluster model. Therefore, periodic DFT calculations were performed for this system. For all four molecules we found good agreement of the adsorption geometry and adsorption energies obtained using the derived force field with the results of our ab initio calculations as well as experimental and theoretical data reported by other authors (Table 4).

The adsorption mechanism of *m*-xylene is very similar to that of benzene. The electrostatic interactions of the negative charge

TABLE 4: Comparison of Cluster HF (for *m*-xylene, dimethyl ether, and benzoic acid) or Periodic DFT (for bi-benzoic acid) Data on the Adsorption Energy and Adsorption Geometry with the Results of Atomistic Calculations, Using the Derived Force Field

		distance, Å		adsorption energy, eV	
molecule		ab initio	atomistic	ab initio	atomistic
m-xylene	C−Ti	3.26	3.00	0.14	0.14
dimethyl ether	O−Ti	2.29	2.25	0.32	0.30
benzoic acid	O−Ti	2.15	2.15	1.30	1.29
bibenzoic acid	O−Ti	2.12	2.03	2.61	2.60

distributed on the aromatic ring with the positive surface Ti ions along with dipole−dipole and dipole−monopole interactions due to polarization of the molecule in the electrostatic field of the surface are the main contributions to the adsorption energy of *m*-xylene. These interactions determine the optimum position of the aromatic ring with respect to the surface with its center above the in-plane Ti ion. In this configuration the methyl groups appear to be positioned above the surface between the in-plane and bridging oxygens, which is energetically unfavorable for these groups, as discussed above. Therefore, the geometry of the adsorption of *m*-xylene is determined by a balance of attractive forces between the aromatic ring and the surface and repulsive forces between the methyl groups of the molecule and the surface O ions. The first interaction tends to bring the molecule parallel to the surface, while the second tends to move it into a perpendicular position. Since the attractive forces are significantly stronger than the repulsive forces, the molecule assumes a configuration with the aromatic ring plane at the angle of 15° to the surface, similar to the results obtained by Susuki et al.[12]

The lowest energy configuration of the dimethyl ether obtained by using the developed force field corresponds to positioning the oxygen of the molecule at 2.25 Å above an in-plane Ti ion and the molecule backbone at 42° to the surface. This configuration arises due to the attraction of the oxygen and carbons of the molecule to the Ti ion in the surface. Therefore in the optimized configuration both C−Ti and O−Ti distances are close to the corresponding equilibrium distances. However, the O−Ti interactions provide the main contribution to the adsorption energy. Therefore, the C−Ti distance for the dimethyl ether is higher than that for methane on the TiO_2 surface, while the O−Ti distance is close to that for the formic acid. The results of our cluster HF and atomistic calculations for the adsorption of dimethyl ether are in reasonable agreement with the results of the MP2 cluster calculations by Borodin et al.[43] However, these authors only used a much smaller cluster consisting of only one Ti and five O atoms to represent the surface. Therefore, the small deviations of our HF and atomistic calculations from the MP2 data may be attributed to the influence of the cluster boundaries on the adsorption of the dimethyl ether.

We have also studied the adsorption of two molecules containing carboxylic groups: benzoic and bibenzoic acids. The calculations for the formic acid showed that dissociative adsorption is energetically more favorable since it allows the formation of relatively strong bonds between both oxygens of the molecule and the surface Ti ions. Therefore, the adsorption of the compounds containing the carboxylic group was modeled for the dissociative mode. The proton from the carboxylic group was positioned on the closest to the adsorbate bridging oxygen of the surface. The geometry of both the molecule and the proton on the surface was optimized. The adsorption geometries for benzoic and bibenzoic acid correspond to the molecules standing upright on the surface with the oxygens of the carboxylic groups above the in-plane Ti ions. They are similar to those obtained for isonicotinic and biisonicotinic acids in ref 46, using periodic boundary conditions and the INDO method. This seems to be natural since the adsorption of these two molecules is largely due to the interaction of the carboxylic group with the rutile surface. Therefore slight variations of the chemical structure of the rest of the molecule, which is further away from the surface, are not crucial. The upright position of benzoic and bibenzoic acids is due to the competition between the following forces: the attraction of both carboxylic and aromatic groups to the in-plane Ti ions, the torsional rigidity of the molecule, and the repulsion of the aromatic ring from the bridging oxygens of the surface. Since the strengths of the attractive interactions of Ti/carboxylic group and Ti/benzyl are different and the strong torsional rigidity of the molecule does not allow for the bending of the molecule to achieve most energetically favorable configurations for both the carboxylic and aromatic groups, only the carboxylic groups assume their optimum position on the surface with the two oxygens above Ti ions. Therefore, the position of the aromatic ring of the benzoic acid is perpendicular to the surface since this configuration minimizes the repulsive interactions with the bridging oxygens. Due to the constraint of the covalent bonding of the aromatic rings in the bibenzoic acid, the aromatic planes are at an angle of 73° to the surface.

5.3. Adsorption of $C_{52}H_{72}O_3$ on TiO_2 (110). These tests clearly demonstrate that the force field derived on the basis of the interactions of small molecules with the rutile TiO_2 (110) surface is able to describe the interactions of more complex molecules consisting of methyl, carboxylic, and aromatic groups with this surface. Therefore, we believe that it can be used for predictive modeling of the properties of a wide variety of organic molecules at the rutile surface. As an example, we have studied the adsorption of the $C_{52}H_{72}O_3$ molecule on the TiO_2 surface (see Figure 1b). Calculations were performed in a cluster model, using a (10×5) unit cell cluster four layers deep to represent the rutile (110) surface. Note that only part of the cluster representing the TiO_2 (110) surface is shown in Figure 1b. The Ti ions at the borders of the cluster carry half of the charge of titaniums inside the cluster. This results in a zero in-plane dipole moment of the cluster and the same electrostatic potential from the surface as in the periodic model.

The molecule consists of three 3,5 isobutyl phenyl headgroups (derivatives of *m*-xylene) and an ethyl formate tail group. Finding a global energy minimum configuration of this molecule on the surface is a complex and separate problem, which is not a topic of the present paper. The equilibration of a large organic molecule on a surface involves both fast vibrations of the molecule's functional groups in local potential minima and slow transitions (translation of the center of mass of the molecule and rotation of its main axes) between the local minima. This multiscale problem can be addressed via kinetic Monte Carlo or accelerated molecular dynamics providing the saddle points of a multidimensional potential surface are known (see, for example, ref 47), and is a topic of our current research. In the present paper we did not study all possible stable configurations of this molecule on a rutile surface, but considered only two most symmetric configurations in order to demonstrate the application of the force field to a larger molecule on the TiO_2 surface. In both configurations the carboxylic group of the molecule's tail is above the in-plane Ti atoms, but in configuration 1 the main axis of the molecule is perpendicular to the surface bridging O rows (Figure 1b), and in configuration 2 it is parallel to the O rows. In both configurations most parts of

the molecule are further than 5 Å from the surface, which results in very weak interactions, electrostatic in nature, between these parts and the surface. Due to the weakness of these molecule/surface interactions and the rigidity of the molecule backbone determined by the tetrahedral arrangement of the bonds of the central sp^3-hybridized carbon and the head/tail groups of the molecule, the relaxation of the molecule on the surface is determined by the soft modes of the molecule. The soft modes of $C_{52}H_{72}O_3$ include the rotational modes of the headgroup methyls and relative flexibility of the carboxylic tail group with respect to rotation of the OCO plane. Therefore, the relaxation of the molecule on the surface mostly involves the adjustment of these groups in the electrostatic field of the surface. The distances of the oxygens of the carboxylic group of the molecule from the in-plane Ti ions are 3.26 and 3.28 Å in configuration 1 and 2, respectively. The lowest carbon of the molecule's methyl group is 4.47 (configuration 1) and 4.12 Å (configuration 2) away from the Ti plane. The adsorption energies in these two configurations are 1.45 (configuration 1) and 1.12 eV (configuration 2), respectively. These adsorption energies are close to the adsorption energy of formate, which equals 1.32 eV. Therefore the adsorption of the $C_{52}H_{72}O_3$ molecule is mostly due to the interactions of the tail carboxylic group with the surface, while the rest of the molecule contributes only slightly to the adsorption energy.

Our preliminary static calculations have shown that there is virtually no barrier for the motion of the molecules along the Ti row in both parallel and transverse configurations. It has been shown experimentally that the molecule is indeed mobile on the surface.[10] We have estimated the barrier for the motion of the molecule perpendicular to the Ti row in the transverse configuration to be 0.7 eV with the highest energy configuration corresponding to the configuration with the tail carboxylic group above the oxygen bridge.

6. Conclusions

In this paper we have studied the adsorption of a number of organic molecules consisting of methyl, benzyl, and carboxylic groups on the rutile TiO_2 (110) surface using both ab initio and atomistic simulation techniques. We have further tested the applicability of a simple embedded cluster model[23,24] to the study of the adsorption of small organic molecules at the rutile TiO_2 (110) surface and used this model to develop a classical force field for the interactions of a wide class of organic molecules consisting of these groups with the rutile TiO_2 (110) surface. The force field accounts for physisorption and ionic bonding of organic molecules at the surface. It is unable to describe covalent bond formation/dissociation, i.e., the processes associated with charge transfer between a molecule and the surface. The force field allows the reproduction of adsorption energies and geometries of organic molecules on the rutile surface. It should be useful for studying diffusion of these molecules and their manipulation with AFM and STM tips.

Our results demonstrate that a separate description of the interactions of individual functional groups of larger molecules with the surface can be used to describe the interactions of whole complex molecules with the surface. However, this procedure is only valid if the electronic structure of the functional groups in the complex molecule does not differ much from the electronic structure of the small molecules representing those groups. For example, as we have shown above, the substitution of the hydrogens in benzene with methyls satisfies this requirement. Aliphatic hydrocarbon chains also can be considered as combinations of methyl groups. However, this approach is less valid for highly conjugated systems such as polycyclic aromatic molecules. These cannot be divided into benzene derivatives since the electronic structure, and therefore the interaction energy with the surface, of the separate parts and the whole molecule can prove to be quite different.

Acknowledgment. We thank Peter Sushko and Jacob Gavartin for useful discussions. We are grateful to Dorothy Duffy, Matt Watkins, and Charles Bird for critically reading the manuscript. M.L.S. and A.Y.G. are grateful to EPSRC and the IRC in Nanotechnology for financial support. We acknowledge the financial support of the EU FP6 project Nanoman. The HPCx computer time was awarded to the Materials Chemistry consortium under EPSRC grant GR/S13422/01.

References and Notes

(1) Groning, P. *Adv. Eng. Mater.* **2005**, *7*, 279.
(2) Nony, L.; Bennewitz, R.; Pfeiffer, O.; Gnecco, E.; Baratoff, A.; Meyer, E.; Eguchi, T.; Gourdon, A.; Joachim, C. *Nanotechnology* **2004**, *15*, S91.
(3) Schnadt, J.; Bruhwiler, P. A.; Patthey, L.; O'Shea, J. N.; Sodergren, S.; Odelius, M.; Ahuja, R.; Karis, O.; Bassler, M.; Persson, P.; Siegbahn, H.; Lunell, S.; Martensson, N. *Nature* **2002**, *418*, 620.
(4) Luo, Y.; Collier, P.; Jeppesen, J. O.; Nielsen, K. A.; Delonno, E.; Ho, G.; Perkins, J.; Tseng, H.-R.; Yamamoto, T.; Stoddart, J. F.; Heath, J. R. *ChemPhysChem.* **2002**, *3*, 519.
(5) Diebold, U. *Surf. Sci. Rep.* **2003**, *48*, 53.
(6) Foster, A. S.; Gal, A. Y.; Nieminen, R. M.; Shluger, A. L. *J. Phys. Chem. B* **2005**, *109*, 4554.
(7) Patthey, L.; Rensmo, H.; Persson, P.; Westermark, K.; Vayssieres, L.; Stashans, A.; Petersson, A.; Bruhwiler, P. A.; Siegbahn, H.; Lunell, S.; Martensson, N. *J. Chem. Phys.* **1999**, *110*, 5913.
(8) Persson, P.; Lunell, S.; Ojamae, L. *Chem. Phys. Lett.* **2002**, *364*, 469.
(9) Persson, P.; Lunell, S. *Sol. Energy Mater. Sol. Cells* **2000**, *63*, 139.
(10) Gauthier, S. Personal communication.
(11) Bandura, A. V.; Kubicki, J. D. *J. Chem. Phys. B* **2003**, *107*, 11072.
(12) Suzuki, S.; Yamaguchi, Y.; Onishi, H.; Sasaki, T.; Fukui, K.; Iwasawa, Y. *J. Chem. Soc., Faraday Trans.* **1998**, *94*, 161.
(13) Sun, H. *J. Phys. Chem. B* **1998**, *102*, 7338.
(14) Sun, H.; Ren, P.; Fried, J. R. *Comput. Theor. Polym. Sci.* **1998**, *8*, 229.
(15) Bunte, S. W.; Sun, H. *J. Phys. Chem. B* **2000**, *104*, 2477.
(16) de Leeuw, N. M. *J. Phys. Chem. B* **2002**, *106*, 5241.
(17) Hwang, S.; Blanco, M.; Goddard, W. A. *J. Phys. Chem. B* **2001**, *105*, 10746.
(18) Cornell, W. D.; Cieplak, P.; Balyly, C. I.; Gould, I. R.; Merz, K. M.; Ferguson, D. M.; Spellmeyer, D. C.; Fox, T.; Caldwell, J. W.; Kollman, P. A. *J. Am. Chem. Soc.* **1995**, *117*, 5179.
(19) Casarin, M.; Maccato, C.; Vittadini, A. *J. Chem. Phys. B* **1998**, *102*, 10745.
(20) Becke, A. D. *J. Chem. Phys.* **1993**, *98*, 5648.
(21) Lee, C.; Yang, W.; Parr, R. G. *Phys. Rev. B* **1988**, *37*, 785.
(22) Frisch, M. J.; Trucks, G. W.; Schlegel, H. B.; Scuseria, G. E.; Robb, M. A.; Cheeseman, J. R.; Zakrzewski, V. G.; Montgomery, J. A., Jr.; Statmann, R. E.; Burant, J. C.; Dapprich, S.; Millam, J. M.; Daniels, A. D.; Kudin, K. N.; Strain, M. C.; Farkas, O.; Tomasi, J.; Barone, V.; Cossi, M.; Cammi, R.; Mennucci, B.; Pomelli, C.; Adamo, C.; Clifford, S.; Ochterski, J.; Petersson, G. A.; Ayala, P. Y.; Cui, Q.; Morokuma, K.; Malick, D. K.; Rabuck, A. D.; Radhavachari, K.; Foresman, J. B.; Cioslowski, J.; Ortiz, J. V.; Baboul, A. G.; Stefanov, B. B.; Liu, G.; Liashenko, A.; Piskorz, P.; Komaromi, I.; Gomperts, R.; Martin, R. L.; Fox, D. J.; Keith, T.; Al-Laham, M. A.; Peng, C. Y.; Nanayakkara, A.; Gonzalez, C.; Challacombe, M.; Gill, P. M. W.; Johnson, B.; Chen, W.; Wong, M. W.; Andres, J. L.; Gonzalez, C.; Head-Gordon, M.; Replogle, E. S.; Pople, J. A. *Gaussian98*; Gaussian, Inc.: Pittsburgh, PA, 1998.
(23) Sulimov, V. B.; Sushko, P. V.; Edwards, A. H.; Shluger, A. L.; Stoneham, A. M. *Phys. Rev. B* **2002**, *66*, 024108.
(24) Sushko, P. V.; Shluger, A. L.; Catlow, C. R. *Surf. Sci.* **2000**, *450*, 153.
(25) Junquera, J.; Paz, O.; Sanchez-Portal, D.; Artacho, E. *Phys. Rev. B* **2001**, *64*, 235111.
(26) Soler, J. M.; Artacho, E.; Gale, J. D.; Garcia, A.; Junquera, J.; Ordejon, P.; Sanchez-Portal, D. *J. Phys.: Condens. Matter* **2002**, *14*, 2745.
(27) Artacho, E.; Sánchez-Portal, D.; García, P. A.; Soler, J. M. *Phys. Status Solidi B* **1999**, *215*, 809.
(28) Fukui, K.; Onishi, H.; Iwasawa, Y. *Appl. Surf. Sci.* **1999**, *140*, 259.

(29) Muscat, J.; Wander, A.; Harrison, N. M. *Chem. Phys. Lett.* **2001**, *342*, 397.
(30) Cronemeyer, D. C. *Phys. Rev.* **1952**, *87*, 876.
(31) Henrich, V. E.; Kurtz, R. L. *Phys. Rev. B* **1981**, *23*, 6280.
(32) Henrich, V. E. *Rep. Prog. Phys.* **1985**, *48*, 1494.
(33) Charlton, G.; Howes, P. B.; Nicklin, C. L.; Steadman, P.; Taylor, J. S. G. *Phys. Rev. Lett.* **1997**, *78*, 495.
(34) Harrison, N. M.; Wang, X.-G.; Muscat, J.; Scheffler, M. *Faraday Discuss.* **1999**, *114*, 305.
(35) Lindan, P. J. D.; Muscat, J.; Harrison, N. M.; Gillan, M. *Faraday Discuss.* **1997**, *106*, 135.
(36) Ramamoorthy, M.; Vanderbil, T. D.; Kingsmith, R. D. *Phys. Rev. B* **1994**, *49*, 16721.
(37) Saunders, V. R.; Dovesi, R.; Roetti, C.; Orlando, R.; Zicovich-Wilson, C. M.; Harrison, N. M.; Doll, K.; Civalleri, B.; Bush, I. J.; D'Arco, Ph.; Lunell, M. L. *Crystal03*, Release 1.0.
(38) Kackel, P.; Terakura, K. *Appl. Surf. Sci.* **2000**, *166*, 370.
(39) Morikawa, Y.; Takahashi, I.; Aizawa, M.; Namai, Y.; Sasaki, T.; Iwasawa, Y. *J. Phys. Chem. B* **2004**, *108*, 14446.
(40) Nilsing, M.; Lunell, S.; Persson, P.; Ojamae, L. *Surf. Sci.* **2005**, *582*, 49.
(41) NIST Computational Chemistry Comparison and Benchmark Database, NIST Standard Reference Database No. 101, Release 11, May 2005, Editor: Russell D. Johnson III; http://srdata.nist.gov/cccbdb
(42) Raza, H.; Wincott, P. L.; Thornton, G.; Casanova, R.; Rodriguez, A. *Surf. Sci.* **1998**, *404*, 710.
(43) Borodin, O.; Smith, G. D.; Bandyopadhyaya, R.; Byutner, O. *Macromolecules* **2003**, *36*, 7873.
(44) Gale, J. D. *J. Chem. Soc., Faraday Trans.* **1997**, *93*, 69.
(45) Press: W. H.; Teukolsky, S. A.; Vetterling, W. T.; Flannery, B. P. *Numerical recipes in Fortran*: *the Art of Scientific Computing*; Cambridge University Press: Cambridge, MA, 1986.
(46) Persson, P.; Stashans, A.; Bergstrom, R.; Lunell, S. *Int. J. Quantum Chem.* **1998**, *70*, 1055.
(47) Miron, R. A.; Fichthorn, K. A. *J. Chem. Phys.* **2001**, *115*, 8742.